ZHUANG, Chaoqun; WANG, Shengwei; SHAN, Kui. A risk-based robust optimal chiller sequencing control strategy for energy-efficient operation considering measurement uncertainties. Applied Energy, 2020, 280: 115983.

https://doi.org/10.1016/j.apenergy.2020.115983

This is the Pre-Published Version.

A risk-based robust optimal chiller sequencing control strategy for energy-efficient operation considering measurement uncertainties

Chaoqun Zhuang, Shengwei Wang* and Kui Shan

Department of Building Services Engineering, The Hong Kong Polytechnic University, Kowloon, Hong Kong

Abstract: Proper and reliable control of central chilling systems with multiple chillers is crucial to save energy and enhance energy efficiency. The conventional total-cooling-load-based chiller sequencing control strategies determine switching (on/off) thresholds according to building instantaneous cooling load and chiller maximum cooling capacity. However, due to the existence of measurement uncertainties and ever-changing operating conditions, optimal switching points often deviate significantly from predefined thresholds. To deal with these challenges and uncertainties, a risk-based robust optimal chiller sequencing control strategy is proposed to improve the robustness and energy efficiency of chillers in operation. As the core of the control strategy, an online stochastic decision-making scheme, which is developed to optimize chiller staging based on quantified risks. The risk of failure to achieve expected operation performance by switching on/off a chiller is evaluated through analyzing the probabilistic fused cooling load and the probabilistic chiller maximum cooling capacity, based on Bayesian calibration of cooling load and capacity models. The best switching points can therefore be identified in a stochastic approach. The results of case studies show that the proposed strategy can improve the reliability and robustness of chiller sequence operation. Compared with the conventional strategy, the switching frequency was decreased by more than 54%, and the energy use of central cooling systems can be reduced by 2.8% without sacrificing thermal comfort.

Keywords: Risk-based control; measurement uncertainty; chiller sequencing; Bayesian calibration; robust optimal control.

* Corresponding author: Shengwei Wang, email: beswwang@polyu.edu.hk

Nomenclature

AHU	air-handling unit
CP_g	gaseous refrigerant specific heat at constant pressure, kJ/(K·kg)
CP_l	liquid refrigerant specific heat at constant pressure, kJ/(K·kg)
C_{rated}	chiller rated capacity (kW)
c_w	specific thermal capacity of water (kJ/kg·°C)
CV(RMSE)	coefficient of variation of the root mean square error
d	dead band
E_{com}	electrical power of chillers (kW)
E	energy consumption (kWh)
h_{fg}	latent heat of vaporization at the reference state pressure (kJ/kg)
j, k	number of samples
M	measured value
MCMC	Markov Chain Monte Carlo
N	number of chillers in operation
N_{mean}	chiller mean stages
P_{cd}	condensing pressure (kPa)
P_{ev}	evaporating pressure (kPa)
q_{fu}	fused cooling load (kW)
q_{max}	maximum cooling capacity (kW)
Q_{fu}	probabilistic fused cooling load (kW)
Q_{max}	probabilistic maximum cooling capacity (kW)
R	gas constant
R_f	risk/failure probability
SN_{tot}	total switching number of chillers
T	temperature (°C)
TH	threshold (kW)
v_w	water volumetric flow rate (L/s)
Z	compressibility factor of the refrigerant

Greek letters

Φ	cumulative density function
δ	constant part of the electromechanical losses (kW)
α	loss factor of the variable part of electromechanical losses
v	maximum volumetric flow rate of the gaseous refrigerant (L/s)
ε	aggregated systematic (bias) error (kW)
θ	unknown parameter
η	normalization constant
β	risk threshold
ζ	total integrated time (h)

Subscripts

chi	chiller
ct	cooling tower
dm	direct measurement
im	indirect measurement
pum	pump
rtn	return chilled water
sup	supply chilled water
tot	total

1 Introduction

1.1 Background

Central cooling systems with multiple chillers are widely used in modern commercial buildings to provide cooling for indoor spaces. As a major energy consumer, chillers can consume over half of the total building electricity use [1], leading to considerable interest in the potential for energy savings. Proper control of multiple chillers is crucial to save energy and enhance system energy efficiency. Chiller sequencing control is a control function that determines the number of chillers to be staged on/off in a given load condition [2]. Optimal chiller sequencing control should provide buildings with sufficient cooling while avoiding energy wastage. Excessive operation of chillers could certainly fulfill demanded cooling load, but would consume more electricity. However, inadequate operation of chillers would fail to provide enough cooling and therefore cause thermal discomfort.

Chiller sequencing control strategies can be categorized into direct or indirect methods according to indicators of building instantaneous cooling loads [3]. The direct method determines the chiller stages based on cooling load directly by measuring supply and return water temperature as well as total chilled water flow. The indirect methods determine the chiller stages based on indirect indicators of cooling load, such as the chilled return water temperature, bypass water flow, chiller vane opening and chiller current/power. The total-cooling-load-based chiller sequencing control strategies (i.e. direct methods) are considered the most promising strategy in principle as the indirect indicators may not be proportional to the cooling load [4]. It is straightforward and convenient to measure cooling loads by the product of the water flow rate and differential chilled water temperature. However, site studies showed that the total-cooling-load-based chiller sequencing control strategy does not always ensure the proper operation of systems because the differential temperature cannot be measured accurately [5]. The accuracy of the direct measurement of cooling loads may be significantly influenced by measurement errors, making no sense for incorporating an energy-efficient chiller sequencing control [6]. For instance, an error of 0.4 °C in the measurement of either supply or return chilled water temperature can lead to an error rate of up to 10% in total cooling load measurement, if the differential temperature is 4 °C. A survey of 30 central chiller plants conducted in Hong Kong also indicated that the measurements of water temperature and flow rate were not reliable/accurate enough for proper sequence operation [7].

Various chiller sequencing control strategies have been developed to handle these uncertainties in cooling load measurement. Sun et al. [8] utilized fused measurements of building cooling loads to improve the reliability of chiller sequencing control, by combining the complementary advantages of both direct and indirect cooling load measurement. Huang et al. [9] developed a strategy of fusing available redundant measurements to improve the accuracy of cooling load measurements and reduce measurement uncertainties using a model-free method. Liao et al. [10] proposed a practical way to enhance the robustness of chiller sequencing control by making use of the complementarity of different load indicators. Apart from the uncertainties in cooling load measurements, the maximum cooling capacity of individual chillers is also difficult to determine as it varies with operating conditions [11]. Conventionally, the rated cooling capacity provided by manufacturers is used as a switching threshold while the difference between the rated and real cooling capacity of chillers can certainly affect chiller operating efficiency. To consider the effects of variations in chiller cooling capacity, Liu et al. [12] used iteration loops to estimate the maximum cooling capacity of individual chillers based on the energy balance between chillers and cooling towers. In addition, data-driven models were adopted by Shan et al. [13] to predict maximum cooling capacity under varying chiller operating conditions. Due to the propagation and interaction of different uncertainty sources in operation, the evaluation of the aggregated uncertainty of a multiple-chiller plant becomes complicated.

Uncertainty information is critical in supporting the decisions for achieving optimal design/control objectives [14]. Decision making based on stochastic programming is one of the effective approaches to improve the estimation accuracy and decision quality in presence of uncertainty [15]. The main advantage of stochastic programming over its deterministic counterpart is that the optimal objective in decision-making process can be obtained in an expected value sense [16]. In addition, this method can also introduce flexibility in decision making according to decision-maker attitudes (e.g. risk-neutral or risk-averse) in responding to possible changes that are uncertain or as yet unknown [17]. With respect to addressing uncertainties, risk assessment with advanced stochastic models [18] has been widely used for balancing between acceptable levels of risk and the costs of further risk reduction [19]. For instance, a multi-stage stochastic optimization model, which involves risk management considering the variability of the uncertain parameters, was developed by Cano et al.

[20] for optimal planning of building energy systems. Chou and Ongkowijoyo [21] proposed a risk-based stochastic graphical matrix model to determine renewable energy system schemes with improved reliability. Mavromatidis et al. [22] proposed a two-stage risk-based stochastic program for sizing cost-optimal distributed energy systems considering the uncertain heat and electricity demands, solar radiation and electricity price. For existing studies, stochastic decision-making approaches are generally developed for the applications in the design or plan stage, while there is lack of feasible online decision-making approach to ensure robust chiller sequencing control considering measurement uncertainties.

1.2 Novelty and main contributions

To reduce/consider the impacts of measurement uncertainties, previous studies mainly focused on improving the accuracy of cooling load measurement and chiller cooling capacity estimations. The operating number of chillers is determined by comparing the deterministic values of cooling load and chiller maximum cooling capacity. Although a stochastic chiller sequencing control strategy is used by Li et al. [23], by quantifying the uncertainties associated with cooling load measurement and chiller cooling capacity with predefined normal/uniform distributions, the parameter settings of the distributions would still significantly affect final decision making.

This study therefore proposes a risk-based robust optimal chiller sequencing control strategy for achieving the energy-efficient operation of chillers considering measurement uncertainties. The main innovation of this strategy is the development of an online stochastic decision-making scheme to optimize chiller switching based on the quantified risks (i.e. failure in achieving expected operation performance). The risks by switching on/off a chiller are quantified and used for decision making, considering changes in operating conditions as well as measurement uncertainties. Probabilistic simplified physical models are developed to determine the distributions of cooling loads and maximum cooling capacities for online risk quantification. The proposed control strategy is developed by addressing the following two tasks: 1) offline uncertain parameter identification in probabilistic models for cooling load/capacity estimations; 2) an online risk-based decision-making scheme to determine optimal chiller stages. The uncertain parameters of the probabilistic models are identified using the Bayesian Markov Chain Monte Carlo (MCMC) method. The risks of switching on/ off a chiller are quantified by analyzing the probabilistic fused cooling load and the probabilistic

chiller maximum cooling capacity. To verify the proposed strategy, case studies are conducted in the tallest building in Hong Kong. The energy performance and control robustness of the proposed strategy are investigated and compared with the conventional total-cooling-load based strategy.

The original contributions of this study are briefly summarized as follows:

1) The chiller sequencing control strategy based on risk assessment with a stochastic manner, to the authors' best knowledge, is proposed for the first time to address the measurement uncertainties, improving the reliability and robustness of chillers in operation.
2) A data fusion approach, as a key element in the online stochastic decision-making scheme, is proposed to merge the two probabilistic cooling load measurements, so as to remove the outliers and reduce the impact of the measurement uncertainties on the determination of chiller staging.
3) A Bayesian Markov Chain Monte Carlo method is adopted to quantify the unknown parameters of probabilistic models, which can take account of the "aggerated uncertainties" that exist in the estimation of the cooling load/capacity.

2 Risk-based robust optimal chiller sequencing control strategy

2.1 Basic idea and major innovation

Fig. 1 shows the schematic diagram of a typical concerned chilled water system, where its water loop is decoupled into primary and secondary distribution loops balanced by a bypass line. In the primary loop, each chiller is interlocked with a constant-speed chiller water distribution pump and a cooling water distribution pump. The chilled supply water from chillers is mixed up, flowing into terminal air handling units (AHUs) in the secondary loop to provide cooling for the spaces. An online decision-making scheme is used to determine chiller staging according to building instantaneous cooling loads and chiller cooling capacities.

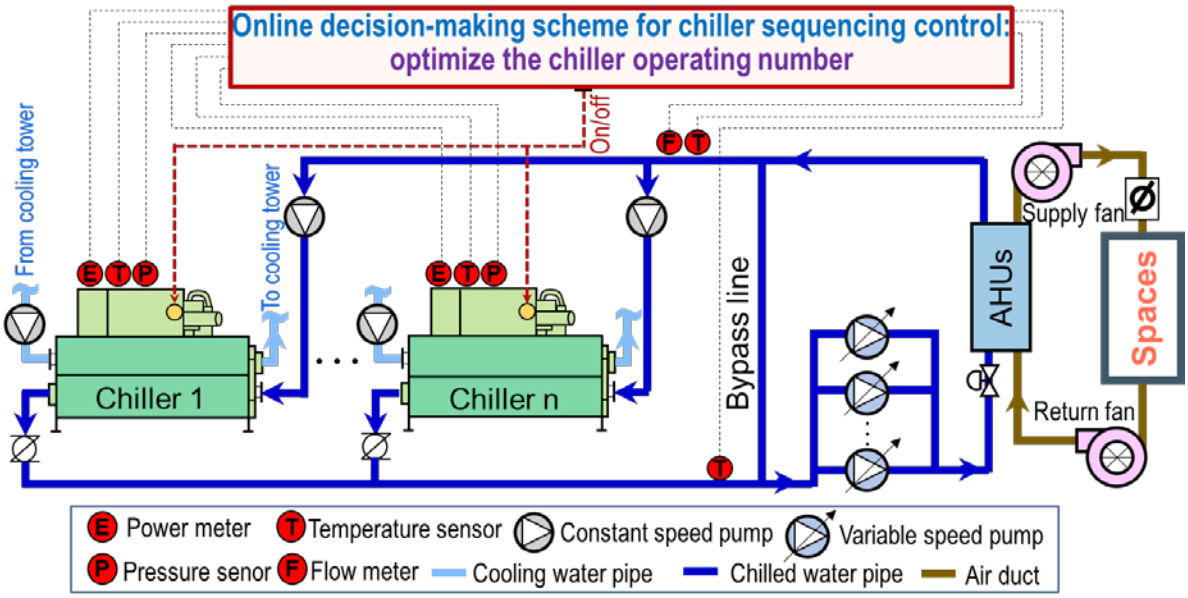

Fig. 1. Schematic diagram of a typical chilled water system

The decision-making schemes of the conventional total-cooling-load-based and proposed risk-based chiller sequencing control strategies are presented in Fig. 2. For the conventional strategy (Fig. 2A), the thresholds for switching on the $(N+1)_{th}$ chiller and switching off the N_{th} chiller, denoted by TH_{on}^{N+1} and TH_{off}^{N}, are normally deterministic, based on the requirement that the maximum cooling capacity provided by chillers should exceed the actual cooling load with minimum energy cost. A dead band d is considered to prevent frequent switching in case the cooling load varies within a small range near the switching points. The cooling load thresholds for switching on/off a chiller are defined by Eq.1 when the chillers are identical. Here, N is the number of chillers in operation. C_{rated} is the rated capacity of chillers (kW). The optimal number of operating chillers can then be determined by Eq.2. The main disadvantage of the conventional strategy is that, under off-design conditions, its switching thresholds may deviate far from the best switching points due to measurement uncertainties and changes in operating conditions (varying chiller maximum cooling capacities).

$$\begin{cases} TH_{off}^{N} = (N-1)\cdot[C_{rated}\cdot(1-d)] \\ TH_{on}^{N+1} = N\cdot[C_{rated}\cdot(1+d)] \end{cases} \tag{1}$$

$$N_{next,con} = \begin{cases} N-1, & Q < TH_{off}^{N} \\ N+1, & Q > TH_{on}^{N+1} \end{cases} \tag{2}$$

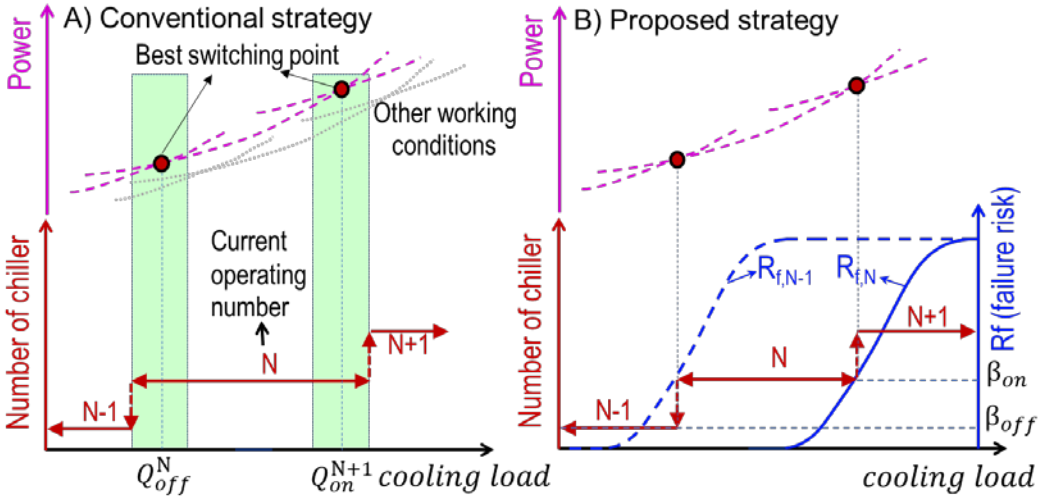

Fig. 2. The basic idea of the proposed risk-based chiller sequencing control and comparison with the conventional strategy

The development of the online stochastic decision-making scheme to determine the chiller staging is the major innovation of the proposed risk-based chiller sequencing control strategy. For the proposed strategy (Fig. 2B), the switching points are determined based on quantifying both the risk (i.e. failure in achieving the expected operation performance) when switching off N_{th} chiller ($R_{f,\,N-1}$) and the risk when operating under current N chillers ($R_{f,\,N}$). The optimal operating number of chillers can then be determined through Eq.3, where β_{on} and β_{off} ($\beta \in [0,\,1]$) are user-defined thresholds and Φ is the cumulative density function (CDF). The risk thresholds (β_{on} and β_{off}) should be properly selected according to the requirements of building thermal comfort and energy efficiency. For a comfort-oriented system requiring sufficient cooling, β_{on} and β_{off} should be set to relatively small values. For an energy-oriented system requiring high energy efficiency, β_{on} and β_{off} should be set to larger values. By adopting the proposed decision-making scheme, the best switching points can always be identified under measurement uncertainties and different operating conditions. Here, $R_{f,\,N-1}$ and $R_{f,\,N}$ are evaluated online by analyzing the probabilistic fused cooling load ($Q_{fu}=[q_{fu,1},\, q_{fu,2},\, \ldots,\, q_{fu,k}]$) and the probabilistic maximum cooling capacity of N-1and N chillers ($Q_{max}^{n-1}=[q_{max,1}^{n-1},\, q_{max,2}^{n-1},\, \ldots,\, q_{max,k}^{n-1}]$ and $Q_{max}^{n}=[q_{max,1}^{n},\, q_{max,2}^{n},\, \ldots,\, q_{max,k}^{n}]$) as presented in Fig. 3. The quantification of fused cooling loads and chiller maximum capacities is further elaborated in Section 2.4.

$$N_{next,new} = \begin{cases} N-1, & R_{f,N-1} = \Phi\left(Q_{fu} > Q_{max}^{N-1}\right) \le \beta_{off} \\ N+1, & R_{f,N} = \Phi\left(Q_{fu} > Q_{max}^{N}\right) \ge \beta_{on} \end{cases} \tag{3}$$

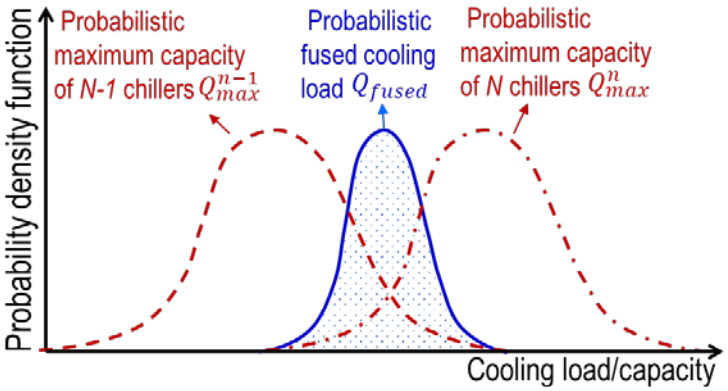

Fig. 3. Probabilistic cooling load and maximum cooling capacity for risk quantification

2.2 Outline of risk-based chiller sequencing control strategy

The outline of the proposed risk-based chiller sequencing control strategy is shown in Fig. 4, which consists of two major tasks to be addressed. The first task is to identify the uncertain parameters of simplified physical models for estimating the cooling load and chiller maximum cooling capacity in an indirect way. A Bayesian Markov Chain Monte Carlo (MCMC) method [24] is used to calibrate the probabilistic models using in-situ measurements. The second task is to quantify the risks of switching on/off a chiller for online decision making. A data fusion approach is developed to fuse the probabilistic direct and indirect cooling loads for outlier removal. The risks are quantified by analyzing the probabilistic fused cooling load and probabilistic chiller maximum cooling capacity. The details to address each task are illustrated in Sections 2.3 and 2.4, respectively.

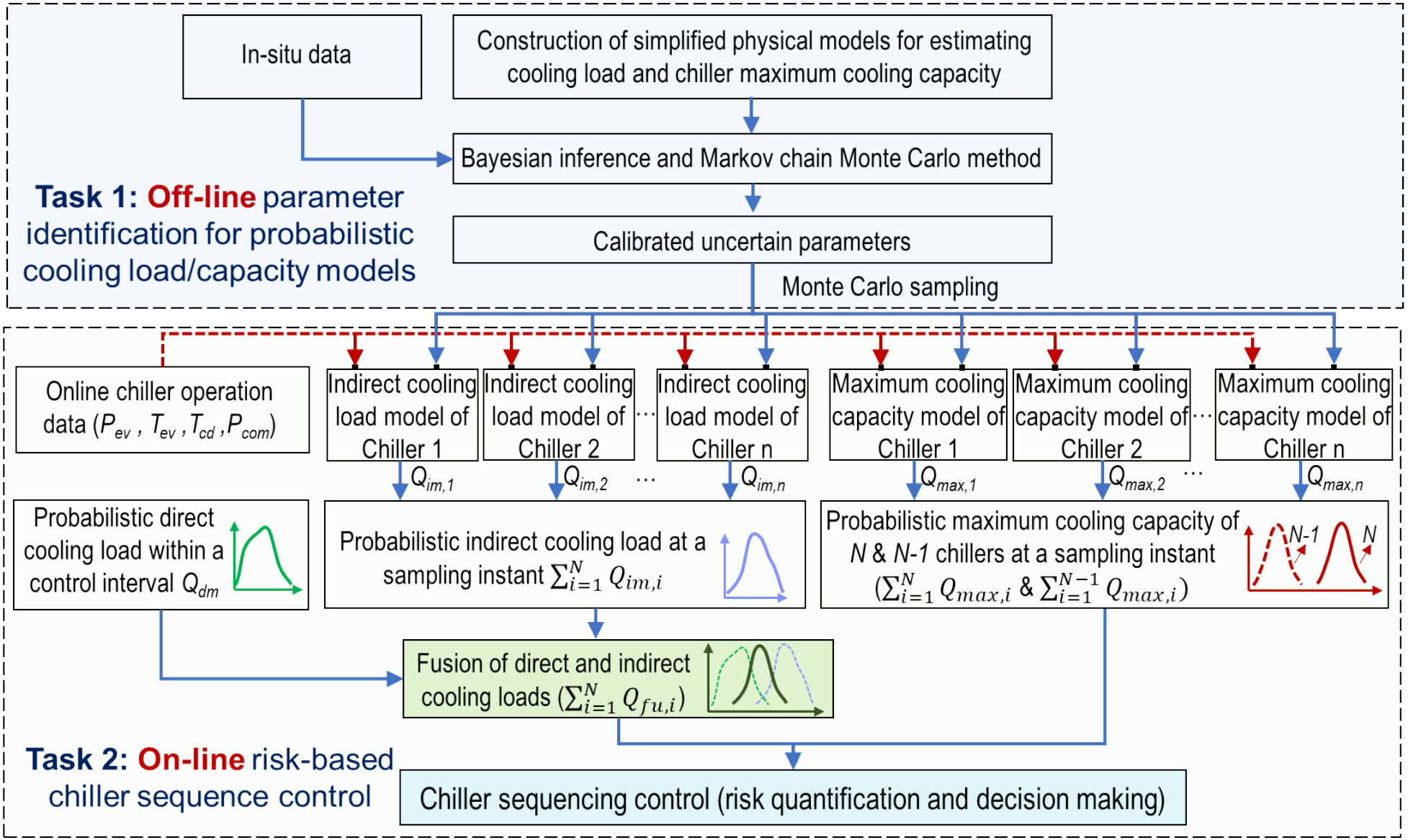

Fig. 4. Framework of the proposed risk-based chiller sequencing control strategy

2.3 Calibration of probabilistic cooling load and maximum cooling capacity models

The building cooling loads can be computed through direct and indirect measurements. Each method has benefits [8]. The direct measurement of building cooling load (q_{dm}) can be formulated as shown in Eq.4. c_w is the specific thermal capacity of water (kJ/kg·°C). v_w is the water volumetric flow rate (L/s). T_{rtn} and T_{sup} are chilled return and supply water temperature (°C) respectively. However, q_{dm} is highly susceptible to measurement uncertainties (especially those associated with T_{rtn} and T_{sup}). To improve the quality of building cooling load measurements, an indirect method using a probabilistic indirect cooling load model (i.e. model-based cooling load measurements), relating building cooling load to measurements from the chiller side, can be beneficial in improving the reliability of cooling load measurements.

$$q_{dm} = c_w \cdot \rho_w \cdot v_w \cdot (T_{rtn} - T_{sup}) \tag{4}$$

Additionally, the maximum cooling capacity of a chiller often deviates from its rated cooling capacity, affecting the decision making of chiller sequence operation. To consider varying chiller cooling capacity under different operating conditions, a probabilistic maximum cooling capacity model, using the full-load operation data from the chiller side, is used to calculate the maximum chiller cooling capacity without an iteration loop.

In this study, two probabilistic simplified physical models, an indirect cooling load model and a maximum cooling capacity model, are developed based on the two deterministic models in reference [8]. The measurement uncertainties are aggregated into the probabilistic models by identifying the model parameters as elaborated below.

2.3.1 Probabilistic simplified physical models for cooling load/chiller cooling capacity estimation

The indirect measurements of cooling load q_{im} and maximum cooling capacity with N operating chillers (q^{n}_{max}) can be computed using two probabilistic simplified physical models as shown in Eqs. 5-6.

$$q_{im} = \sum_{i=1}^{N} f_i(E_{com,i}, T_{cd,i}, T_{ev,i}) = \sum_{i=1}^{N} \left[\frac{E_{com,i} - \delta_i}{\alpha_i \cdot CP_g (T_{ev,i} - T_{cd,i})} \left(CP_l \cdot T_{cd,i} - h_{fg} - CP_g \cdot T_{ev,i} \right) \right] + \varepsilon_N \tag{5}$$

$$q^{N}_{max} = \sum_{i=1}^{N} f_i(P_{ev,i}, T_{cd,i}, T_{ev,i}) = \sum_{i=1}^{n} \left[\frac{v_i \cdot P_{ev,i}}{R \cdot Z \cdot (273.15 + T_{ev,i})} \left(h_{fg} + CP_g \cdot T_{ev,i} - CP_l \cdot T_{cd,i} \right) \right] + \varepsilon_N \tag{6}$$

Here, α is the loss factor of the variable part of electromechanical losses. δ is the constant part of the electromechanical losses (kW). h_{fg} is the latent heat of vaporization at the reference state pressure (kJ/kg). CP_g is the gaseous refrigerant specific heat at constant pressure in kJ/(K·kg). CP_l is the liquid refrigerant specific heat at constant pressure in kJ/(K·kg). E_{com} is the electrical power of chillers (kW), which can be measured directly. T_{cd} and T_{ev} are condensing temperature and evaporating temperature derived according to the corresponding condensing pressure P_{cd} and evaporating pressure P_{ev} (kPa). v is the maximum volumetric flow rate of the gaseous refrigerant (L/s). ε is an aggregated systematic (bias) error term (kW), which can be determined under different numbers of operating primary chilled water pumps. R is the gas constant. Z is the compressibility factor of the refrigerant. α, δ, v and ε are unknown parameters to be determined using in-situ measurements. It is worth noting that the unknown parameters (e.g. α, δ and v) of the simplified physical models used in [8] are deterministic values while the parameters used in this study were quantified with certain distributions.

Compared with direct cooling load measurements, the indirect measurements of cooling loads q_{im} are generally reliable. As the condensing temperature and evaporating differential temperature ($\dot{T}_{ev}$-$\dot{T}_{cd}$) have a much larger scale (i.e. over 20°C) than return and supply water differential temperature ($\dot{T}_{rtn}$-$\dot{T}_{sup}$), the effects of associated measurement noises on indirect measurements (Eq.5) are much smaller than that on the direct measurements (Eq.4).

2.3.2 Identification of model parameters using Bayesian Markov Chain Monte Carlo method

The Bayesian MCMC method is employed to calibrate uncertain parameters in the model using the in-situ data, containing two stages: Bayesian inference and MCMC sampling. The Bayesian inference derives the posterior distributions for the calibrated parameters (i.e. α, δ, v and ε) using prior information and observed data, while MCMC sampling is used to generate equivalent samples from the posterior distributions. The equivalent samples represent the numerical approximations of the posterior distributions, and thus they can be used to represent the features of unknown parameters.

Bayesian inference: Given a model $y = f(\theta)$ and the measured data of y, where θ is the unknown parameter to be determined and y is the output, the Bayesian inference deduces the posterior probability $P(\theta|y)$ through Eq.7. Here $P(y|\theta)$ is the likelihood of the measured data y occurring given the input parameter θ. $P(\theta)$ is the prior probability that describes the probability of θ occurring

computed before the collection of in-situ data. $P(y)$ is a normalization constant. In this study, the cooling load q_{im} and maximum cooling capacity of chillers q_{max} are the output y. q_{im} and q_{max} are calculated through Eq.4 using the in-situ data of v_w, T_{rtn} and T_{sup}. The in-situ data of E_{com}, P_{ev}, T_{cd} and T_{ev} as well as the corresponding q_{im} and q_{max} values are used for generating the likelihood based on Eqs.5-6. Notably, the chiller full-load operation data (i.e. chiller vane opening/current higher than high thresholds) are selected for calculating q_{max}, while both the chiller part-load and full-load operation data are selected for calculating q_{im}.

$$P(\theta|y) = P(y|\theta) \cdot P(\theta)/P(y) \propto P(y|\theta) \cdot P(\theta) \quad (7)$$

<u>*Markov chain Monte Carlo (MCMC) sampling:*</u> MCMC, specifically the Metropolis-Hastings algorithm [25], is employed to draw random samples from the joint multivariate posterior distribution. As a result, a sequence of samples with size m, $\{\theta^{(1)}, \theta^{(2)}, ..., \theta^{(m)}\}$ which approximates the theoretical posterior probability density functions (pdfs) of calibration parameters can then be collected. More details for the MCMC sampling method are elaborated in the literature [26].

It is worth noting that, since two probabilistic models were trained using the same sources of measurements, the risks of switching on/off a chiller (Eq.3), determined based on the differential of cooling loads and cooling capacities, can always be reliably quantified in the face of measurement uncertainties.

2.4 Online stochastic decision-making scheme for chiller sequencing control

The online stochastic decision-making scheme for determining the chiller stages involves three steps as follows.

The first step is to obtain the samples of indirect and direct cooling load measurements as well as the maximum cooling capacities of chillers. At each control interval, the indirect cooling loads (Q_{im}=[$q_{im,1}$, $q_{im,2}$, …, $q_{im,k}$]), the maximum cooling capacities with current operating chillers (Q^{n}_{max}=[$q^{n}_{max,1}$, $q^{n}_{max,2}$, …, $q^{n}_{max,k}$]) and the maximum cooling capacities when switching off a chiller (Q^{n-1}_{max}=[$q^{n-1}_{max,1}$, $q^{n-1}_{max,2}$, …, $q^{n-1}_{max,k}$]) are calculated/sampled k times adopting the probabilistic simplified physical models (Eqs.5-6). j samples of direct cooling load measurements (Q_{dm}=[$q_{dm,1}$, $q_{dm,2}$, …, $q_{dm,j}$]) within the control interval were also selected, assuming the building cooling load is relatively stable in a short period.

In the second step, to enhance the robustness of building cooling load measurements, a data fusion approach is used to capitalize on the benefits of direct and indirect cooling load measurements, removing the measurement errors and model errors simultaneously. The probability density function of fused cooling loads (f_{fu}) is computed by the product of two distributions (i.e. direct and indirect cooling load measurements) as shown in Eq.8, where f_{dm} and f_{im} are probability density functions of Q_{dm} and Q_{im} respectively and η is a normalization constant (expressed by Eq.9). The fused cooling loads (Q_{fu}=[$q_{fu,1}$, $q_{fu,2}$, …, $q_{fu,k}$]) are then sampled k times given f_{fu}. Notably, if the direct measurements deviate far from the indirect measurements (i.e. f_{dm}·f_{im} is a null distribution), indicating the indirect measurements may suffer significant model errors (usually occurring at the very start of chiller switching on/off), the f_{fu} is set as f_{dm}. The use of fused cooling loads instead of direct/indirect cooling loads has two benefits. 1) When a direct measurement suffers incidentally from large random errors (marked as "outlier") in a control interval, this outlier can be removed as its probability of occurrence is near zero in f_{im}. 2) When an indirect measurement suffers from large model errors, this outlier can be removed as its probability of occurrence is near zero in f_{dm}.

$$f_{fu}(x) = \begin{cases} \eta \cdot f_{dm}(x) \cdot f_{im}(x) & if: f_{dm}(x) \cdot f_{im}(x) \neq null \\ f_{dm}(x) & if: f_{dm}(x) \cdot f_{im}(x) = null \end{cases} \quad (8)$$

$$\eta = \frac{1}{\int f_{dm}(x) \cdot f_{im}(x) dx} \quad (9)$$

In the third step, the chiller stages can be determined based on quantified risks through Eq.3, using $f_{X_1}(X_1)$ and $f_{X_2}(X_2)$. Here, the probability density function of X_1 ($f_{X_1}(X_1)$) is the convolution of f_{fu} and f^{n}_{max} as expressed by Eq.10, where X_1=Q_{fu}-Q^{n}_{max} and f^{n}_{max} is the probability density function of Q^{n}_{max}. The probability density function of X_2 ($f_{X_2}(X_2)$) is the convolution of f_{fu} and f^{n}_{max} as described by Eq.11, where X_2 =Q_{fu}-Q^{n-1}_{max} and f^{n-1}_{max} is the probability density function of Q^{n-1}_{max}.

$$f_{X_1}(X_1) = \int f_{fu}(X_1 + y) \cdot f^{n}_{max}(y) dy \quad (10)$$

$$f_{X_2}(X_2) = \int f_{fu}(X_2 + y) \cdot f^{n-1}_{max}(y) dy \quad (11)$$

3 Building air-conditioning system and arrangement of online validation tests

3.1 Description of the air-conditioning system

The central cooling system concerned in this study is a complex primary-secondary chilled water system in the tallest building in Hong Kong, where the cooling is dominated throughout a year [27].

The building has a height of 490 m and consists of 108 floors with around 321,000 m^2 floor area. Table 1 shows the specifications of the main equipment in the central cooling system. Six centrifugal chillers with a rated coefficient of performance (COP) of 5.17 are equipped, providing the designed chilled water supply temperature of 5.5 °C. Each chiller is interlocked with a constant-speed chilled water pump (rated flow rate of 375 L/s) and a constant-speed cooling water pump (rated flow rate of 410 L/s). The heat rejection system consists of eleven cooling towers with a total design capacity of 51,709 kW.

Table 1 Specifications of main equipment in the system.

Equipment	Number	Rated capacity (kW)	Flow rate (L/s)	Power (kW)	Head (kPa)
Chiller	6	7,230	-	1,346	-
Cooling tower A	6	5,234	-	152	-
Cooling tower B	5	4,061	-	120	-
Chilled water pump	6	-	345.0	126	31.6
Cooling water pump	6	-	410.1	202	41.6

3.2 TRNSYS-MATLAB co-simulation testbed and test conditions

To test the effectiveness of the proposed strategy, a virtual simulation platform was constructed based on the configuration of the studied central cooling system using a Transient Simulation Program TRNSYS 18 [28]. To take advantage of its powerful computational capabilities, MATLAB was used to program the supervisory controller (i.e. risk-based chiller sequencing control strategy) and was embedded in TRNSYS. The dynamic processes of hydraulics, heat transfer, water flow/pressure balancing, energy conservation and control were simulated for the entire system. The models used in the test platform were calibrated using on-site operational data [29][30]. A simplified global air handling unit (AHU) was built to provide cooling for a thermal building. The “multi-zone building model” type 56 (i.e. the thermal building) in TRNSYS was employed to simulate the thermal behavior of the selected building. The building model in type 56 is a non-geometrical balance model with one air node per zone, representing the thermal capacity of the zone air volume and capacities which are closely connected with the air node [28]. The envelope construction and thermal properties were set satisfying the requirements of the building design description and local energy efficiency standard [31]. The building’s thermal performance and dynamics under the influences of weather, occupancy,

and air-conditioning systems were then characterized.

The actual cooling load data (without measurement uncertainties) used in the case study were generated using a typical cooling load profile of the selected building in 7 days, as presented in Fig. 5. To test the robustness of the proposed control strategy, measurement uncertainties (including biases and noises) were set for different types of sensors in two cases, as summarized in Table 2. Case 1 represents the conditions where the measured cooling loads are higher than actual cooling loads while Case 2 represents the conditions where the measured cooling loads are lower than actual cooling loads.

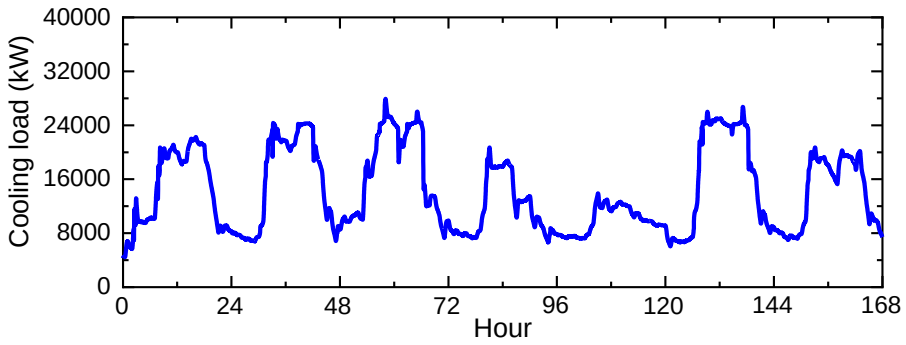

Fig. 5. The actual cooling loads used in the test

Table 2 Sensor noises and biases introduced for case studies.

Measurement	Unit	Bias	Noise
Supply water temperature	°C	**Case 1: -0.4; Case 2: 0.4**	N (0, 0.1)
Return water temperature	°C	**Case 1: 0.2; Case 2: -0.2**	N (0, 0.1)
Supply water flowrate	L/s	Both cases: 20	N (0, 8)
Chiller condensing temperature	°C	Both cases: -0.3	N (0, 0.1)
Chiller evaporating temperature	°C	Both cases: 0.2	N (0, 0.1)

4 In-situ validation of calibrated probabilistic cooling load and capacity models

In this study, 525,600 sets of in-situ measurements (listed in Table 3), obtained from the central cooling systems of the selected high-rise building with the 1-minute interval in 2019, were used to calibrate and validate the models.

The data of Groups 1-21 from 1 July to 31 July were used to identify the parameters of probabilistic indirect cooling load models, while these groups of data from 3 Aug to 10 Aug were used to validate these models. The chiller full-load operation data in the first half-year were used to identify the

parameters of maximum cooling capacity models while the latter half-year data were used to validate these models. The chiller full-load operation data were selected by identifying whether the current and vane opening of the chillers were larger than 70 amperes and 95% respectively. These data were considered observation evidence and were used for producing the likelihood functions. The refrigerant used in the chiller is R134a. The constants used in the model are $R \cdot Z$: 73.41 kJ/(kg·K); h_{fg}: 197.9 kJ/kg; CP_g: 0.89 kJ/(kg·K) and CP_l: 1.27 kJ/(kg·K).

Table 3. In-situ data type and variables.

No.	Measurement	Unit	Symbol
1	Return chilled-water temperature	°C	T_{rtn}
2	Supply chilled-water temperature	°C	T_{sup}
3	Total water volumetric flowrate	L/s	v_w
4-9	Electrical power of chillers 1-6	kW	$E_{com,i}$ (i=1,2,3,4,5,6)
10-15	Condensing pressure of chillers 1-6	°C	$P_{cd,i}$ (i=1,2,3,4,5,6)
16-21	Evaporating pressure of chillers 1-6	°C	$P_{ev,i}$ (i=1,2,3,4,5,6)
22-27	Current of chillers 1-6	A	I_i (i=1,2,3,4,5,6)
28-35	Vane opening of chillers 1-6	%	$VA_{,i}$

A total of 21 uncertain parameters in six indirect cooling load models and six chiller maximum cooling capacity models need to be identified. Here, α_i, δ_i and v_i were set ($i=1,2,3,4,5,6$) as uniform distributions while ε_n ($n=1,2,3$) were set as normal distributions. Notably, the maximum value of n is 3 because the maximum operating number of chillers was 3 in the operating period. Due to a lack of prior knowledge of those uncertain parameters, the deterministic values calculated by the nonlinear least-square method [32] based on Eqs.5-6 with in-situ measurements, were assigned as the mean values of the prior distributions. The lower/upper limits of α_i, δ_i and v_i were assumed to be a deviation of 15% from their corresponding mean values. The standard deviation of ε_n was set as a 5% random error [33].

The detailed information for prior distributions of uncertain parameters can be found in Table 4. A total of 50,000 MCMC simulations were performed while the first 10,000 samples were discarded as a burn-in period. Fig. 6 shows the calibrated distributions of 21 uncertain parameters. Generally, the posterior distribution becomes irregular if the prior distribution follows a uniform distribution, while the posterior distribution nearly follows a normal distribution if the prior distribution follows a normal distribution. Table 4 also lists the characteristic values of the calibrated distributions to be

used for comparing with their prior distributions. The mean values of parameters did not change much after calibration, but the occurrence probability of the values shifted dramatically (e.g. especially for the parameters following uniform distributions). Overall, the calibration process changed the prior information and made the distributions of parameters more informative.

Table 4. Prior and posterior distributions of uncertain parameters.

No.	Parameter	Unit	Prior distribution		Posterior distribution	
			Distribution	Mean	Mean	[25%, 75%]
1	α_1	-	U [0.31,0.41]	0.36	0.36	[0.34,0.38]
2	δ_1	kW	U [621,841]	731	734	[713,750]
3	v_1	L/s	U [1990,2692]	2341	2361	[2322,2402]
4	α_2	-	U [0.26,0.36]	0.31	0.31	[0.29,0.32]
5	δ_2	kW	U [610,825]	718	716	[699,745]
6	v_2	L/s	U [2053,2777]	2415	2362	[2323,2401]
7	α_3	-	U [0.44,0.60]	0.52	0.52	[0.49,0.53]
8	δ_3	kW	U [485,657]	571	568	[553,582]
9	v_3	L/s	U [1958,2650]	2304	2288	[2171,2407]
10	α_4	-	U [0.33,0.44]	0.38	0.38	[0.36,0.40]
11	δ_4	kW	U [559,757]	658	656	[640,671]
12	v_4	L/s	U [1557,2106]	1832	1823	[1791,1863]
13	α_5	-	U [0.30,0.40]	0.35	0.36	[0.34,0.38]
14	δ_5	kW	U [579,783]	681	683	[668,698]
15	v_5	L/s	U [1927,2608]	2268	2302	[2253,2249]
16	α_6	-	U [0.43,0.59]	0.51	0.51	[0.49,0.53]
17	δ_6	kW	U [453,613]	533	534	[520,546]
18	v_6	L/s	U [453,613]	2315	2326	[2190,2421]
19	ε_1	kW	N [536,27]	536	542	[528,557]
20	ε_2	kW	N [977,49]	977	978	[960,995]
21	ε_3	kW	N [1576,78]	1555	1576	[1550,1601]

Note: U represents a uniform distribution and N represents a normal distribution

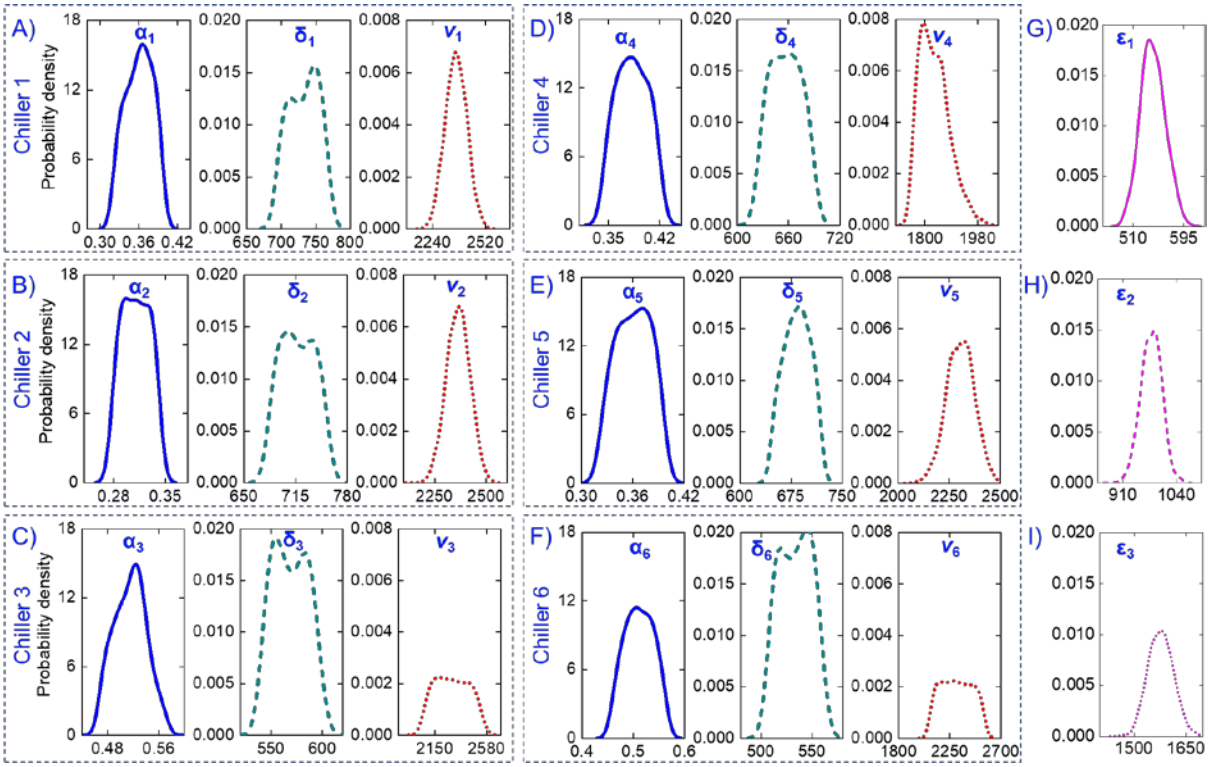

Fig. 6. Distributions of identified parameters of simplified probabilistic physical models

To show the predictive ability of the probabilistic simplified physical models with calibrated parameters (posterior information), the probabilistic indirect cooling load and maximum cooling capacity, calculated by the calibrated models (i.e. 2,000 samples at each sampling instant), are compared with in-situ data as shown in Fig. 7 and Fig. 8. The figures on the right present the probability distributions of the indirect cooling load and maximum cooling capacity in a selected sampling instant. The coefficient of variation of the root mean square error CV(RMSE) [34] was used to evaluate the similarity between the model estimated values and actual values, as shown in Eq.11. The range of CV(RMSE) lies between 0 and 100%, with lower values signifying a good fit between the model and data. Here M_i and $\bar{E}_i$ are the measured and model estimated mean values at i_{th} sampling instant respectively. The measured average values of the cooling load/capacity are denoted by $\bar{M}$.

$$CV(RMSE) = \frac{\sum_{i=1}^{n}(M_i - \bar{E}_i)^2}{\bar{M}} \quad (12)$$

By calculating the index of agreement between model estimated mean and measured cooling load/capacity, it is found that CV(RMSE) for probabilistic cooling/capacity models were 7.5% and 2.9%, respectively. It can be seen that most of the measured load/capacities fell in the 95% prediction intervals. This confirms that the calibrated probabilistic simplified models are satisfactory, and can

be used to reliably estimate the cooling load/capacity.

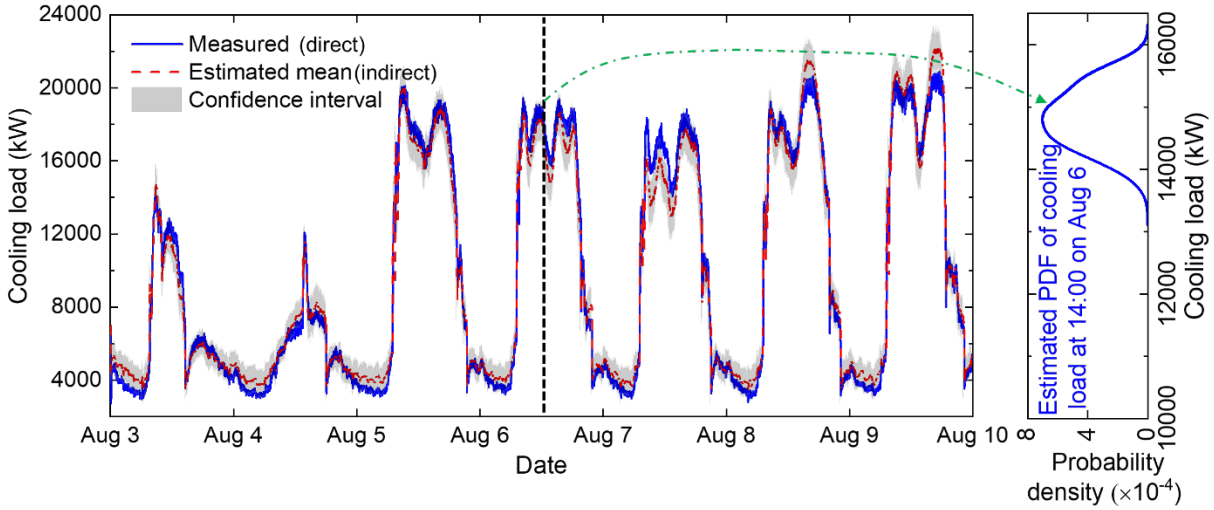

Fig. 7. Indirect measurements of cooling loads using a probabilistic indirect cooling load model *vs* direct measurements (3-10/Aug/2019)

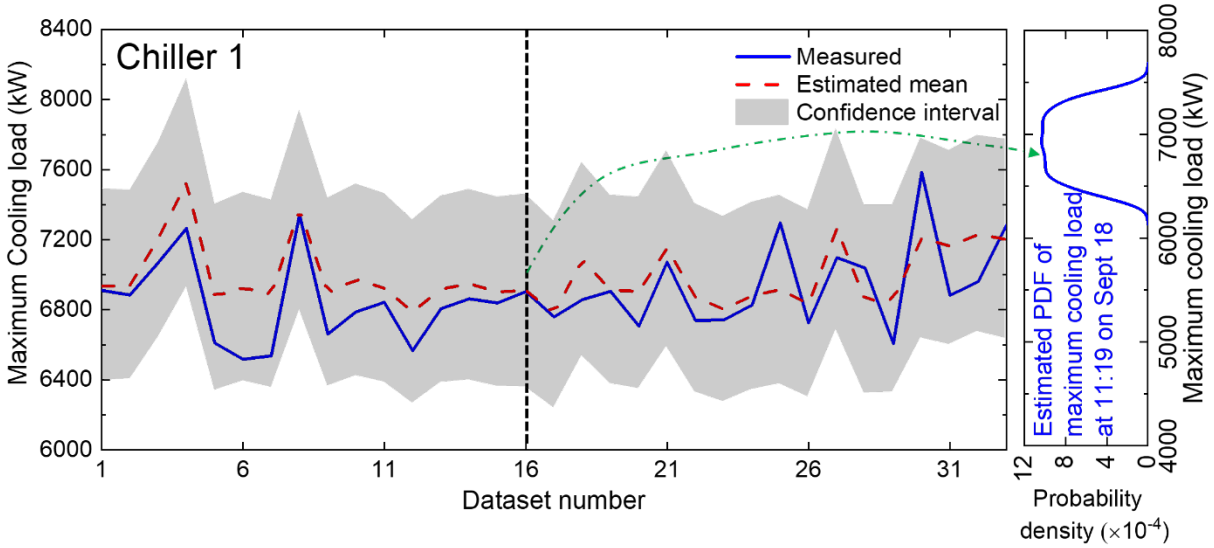

Fig. 8. Estimated maximum cooling capacity using maximum cooling capacity model of chiller 1 *vs* real measurements (July-Dec/2019)

5 Online operation performance and validation of proposed sequence strategy

The control performance and energy efficiency of the central cooling system using the conventional strategy and proposed risk-based chiller sequencing control strategy were evaluated in a virtual simulation platform. The normal operational data were generated for re-calibrating model parameters by simulating the central cooling systems over a wide range of operating conditions considering measurement uncertainties.

The chiller sequencing control algorithm was used in the case study with the following settings:

- Both the simulation time step and the sampling interval of measurements were set 1 second, while the control interval to determine the chiller switching on/off was 5 mins.
- The samples (j) of direct cooling load measurements were set as 60 (i.e. 1-minute data before the control execution). The samples (k) of indirect and fused cooling loads were set as 2,000.
- The dead band d was set as 0.05 (Eq.1) for the conventional strategy.
- Risk thresholds (β_{on} and β_{off}) were set as 0.3 and 0 respectively for the proposed strategy.

Four performance indicators, including the total energy consumption EC_{tot}, total switching number SN_{tot}, chiller mean stages N_{mean} and total integrated time ($\zeta_{0.5}$) where the thermal building's average temperature deviated 0.5 °C from its setpoint (23 °C), were used to evaluate the performance of the chiller sequencing control strategies. The total energy consumption EC_{tot} includes the energy use of chillers (EC_{chi}), constant-speed pumps (EC_{pum}) and cooling towers (EC_{ct}).

5.1 Results of Case 1: measured cooling loads > actual cooling loads

Fig. 9 shows the comparison of direct, indirect and fused measurements of cooling loads in Case 1. There are few outliers in the direct and indirect measurements, also marked in the figure. Two outliers in the direct measurements (i.e. around 83.5 h and 112 h) mainly resulted from large random errors while the outliers in the indirect measurements mainly resulted from model errors (e.g. around 2.3 h and 32.8 h), appearing during very early periods of chiller staging. The use of fused measurements can take advantage of direct and indirect measurements. The outliers or the strikes were efficiently removed, which can avoid unnecessary chiller switching.

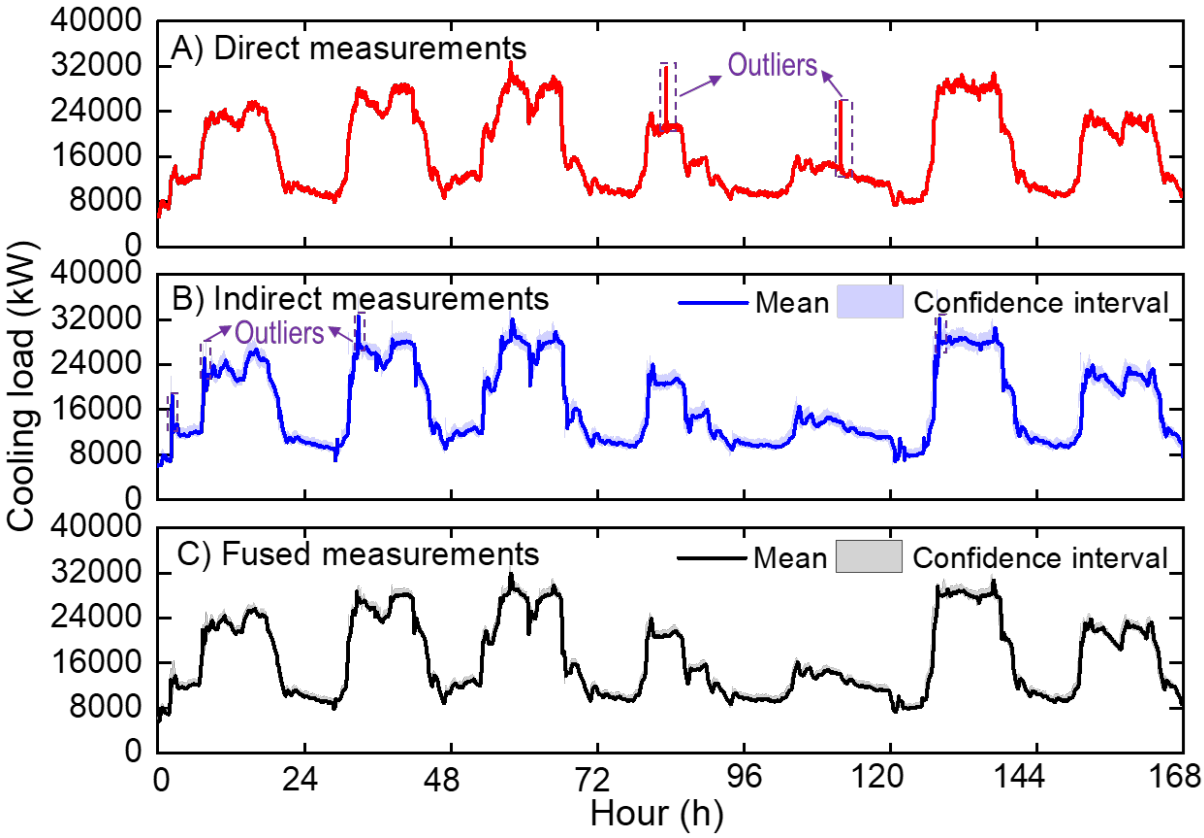

Fig. 9. Comparison on direct, indirect and fused measurements of cooling load

The variation in the number of operating chillers adopting the conventional and proposed strategies are compared and presented in Fig. 10A. It can be seen that the number of chillers in operation varied frequently when adopting the conventional strategy. However, the switching frequency was significantly reduced when adopting the proposed strategy. In addition, the operating number of chillers adopting the conventional strategy was no lower than those adopting the proposed strategy in the test period, due to overestimation of the cooling loads. Fig. 10B shows the indoor temperature of the two strategies. When adopting the proposed strategy, the reduction of chiller operating numbers in some periods would not affect the indoor temperature control (i.e. sufficient cooling can be provided). As listed in Table 5, compared with the conventional strategy, the total switch number SN_{tot} adopting the proposed strategy was decreased by 54% (63 vs. 29). The chiller mean stages in the test period adopting the proposed strategy (i.e. 2.55) were also less than that of the conventional strategy (i.e. 2.84), indicating the potential energy saving. Compared with the conventional strategy, the total energy consumed by the proposed strategy was reduced by 2.8%, without sacrificing indoor thermal comfort (i.e. $\zeta_{0.5}$ was the same in two strategies).

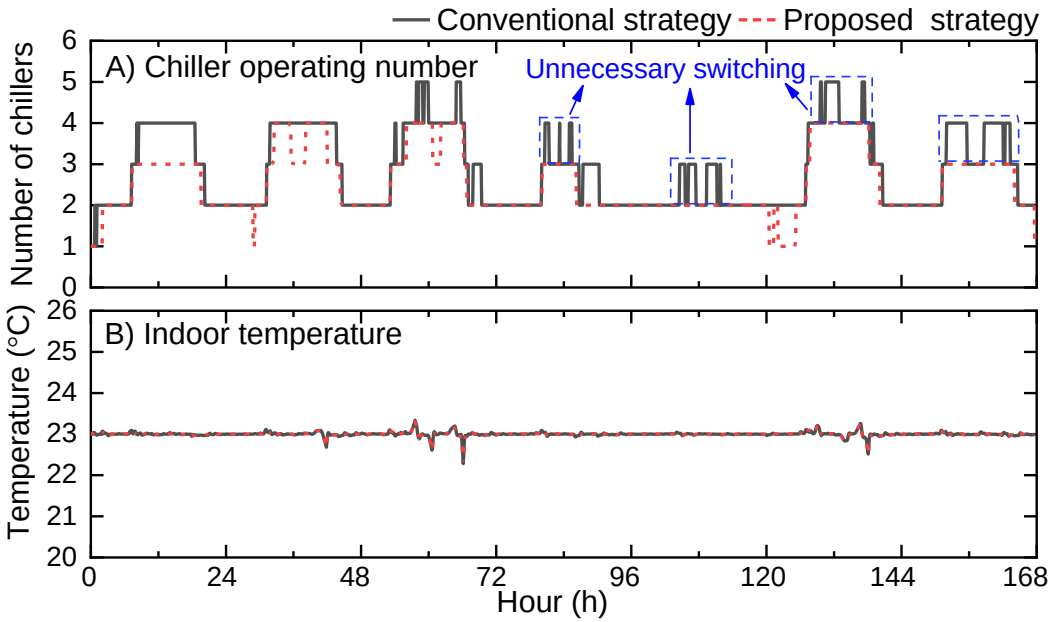

Fig. 10. Control performance of the proposed and conventional strategies in Case 1: A) chiller operating number B) indoor temperature of the thermal building

Table 5 Control performance of proposed and conventional strategies in Case 1

Strategy	SN_{tot}	N_{mean}	EC_{chi} (kWh)	EC_{pum} (kWh)	EC_{ct} (kWh)	EC_{tot} (kWh)	$\zeta_{0.5}$ (h)
Conventional	63	2.84	5.00×10^5	1.4×10^5	7.88×10^4	7.20×10^5	0.18
Proposed	29	2.55	4.99×10^5	1.26×10^5	7.54×10^4	7.00×10^5	0.18

Fig. 10 presents the quantified risks in the decision-making process when adopting the proposed strategy. When the quantified risk operating under N (i.e. current operating number) chillers ($R_{f,N}$) is higher than β_{on} (0.3), an additional chiller would be switched on. When there is no risk of switching off a chiller (i.e., $R_{f,N-1}$=0), one chiller would be staged off. The decision making is conducted based on risk assessment, offering a promising means for engineers to exploit the potential benefits/flexibility of chiller sequencing control.

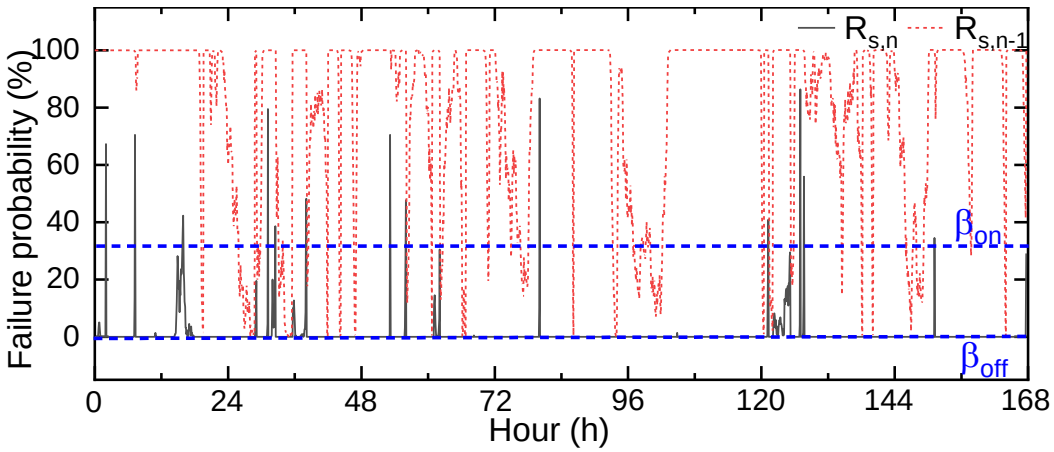

Fig. 11. Quantified risks in the decision-making process of Case 1

5.2 Results of Case 2: measured cooling loads < actual cooling loads

Fig. 12A presents the variation in the number of the operating chillers adopting the conventional and proposed strategies in Case 2, where the measured cooling loads were lower than actual cooling loads. As in Case 1, the number of the operating chillers varied frequently when adopting the conventional strategy, while the switching frequency was significantly reduced when adopting the proposed strategy. However, in contrast to Case 1, the operating number of chillers adopting the conventional strategy was no higher than that of adopting the proposed strategy in the test period, due to underestimation of cooling loads. Fig. 12B shows the indoor temperature under the two different strategies. The reduction of chiller operating numbers in some periods resulted in temperature rise (from 133 h to 138 h) due to insufficient cooling supply under the conventional strategy, while the indoor temperature was well controlled under the proposed strategy. As also listed in Table 6, compared with the conventional strategy, the total switch number SN_{tot} under the proposed strategy decreased dramatically by 82% (194 vs. 35). With the conventional strategy, total energy consumption can be reduced by 1.1% by sacrificing indoor thermal comfort (i.e. indoor temperature cannot be controlled at the desired setpoint). $\zeta_{0.5}$ of the conventional chiller sequencing control was 5.6 h, which was reduced to 0.18 h by the proposed strategy, decreasing by 96.8%.

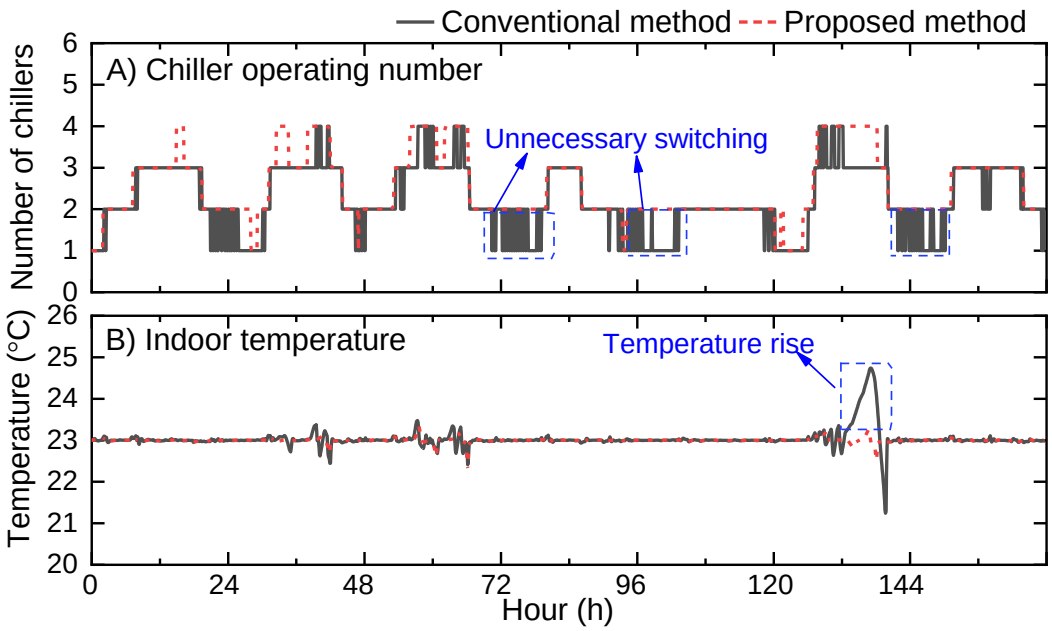

Fig. 12. Control performance of the proposed and conventional strategies in Case 2: A) chiller operating number B) indoor temperature of the thermal building

Table 6 Control performance of proposed and conventional strategies in Case 2

Strategy	SN_{tot}	N_{mean}	EC_{chi} (kWh)	EC_{pum} (kWh)	EC_{ct} (kWh)	EC_{tot} (kWh)	$\zeta_{0.5}$ (h)
Conventional	194	2.23	5.07×10^5	1.10×10^5	7.30×10^4	6.90×10^5	5.60
Proposed	35	2.53	4.98×10^5	1.25×10^5	7.53×10^4	6.98×10^5	0.18

Fig. 13 presents the quantified risks in the decision-making process when adopting the proposed strategy. Compared with Case 1, even the settings of senor bias were different, risk-based decision making can operate the chillers while maintaining both energy-efficiency and robust controls, as the optimal switching points can always be identified under measurement uncertainties and different operating conditions.

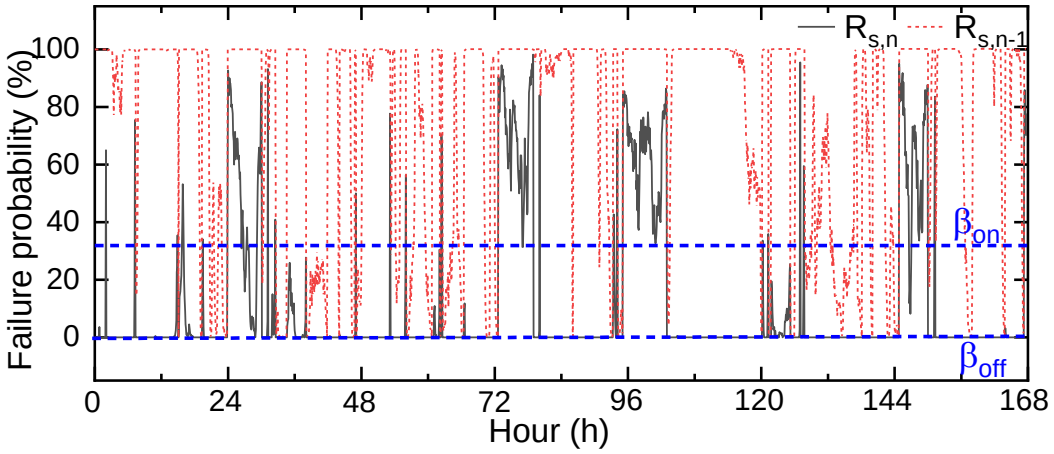

Fig. 13. Quantified risks in the decision-making process in Case 2

6 Conclusions

A risk-based chiller sequencing control strategy was proposed to improve the robustness and energy efficiency of chillers in operation. As the core of the control strategy, an online stochastic decision-making scheme was developed to optimize chiller staging. The risks of switching on/ off a chiller were evaluated based on the probabilistic fused cooling load and the probabilistic chiller maximum cooling capacity. The cooling load and cooling capacity estimation models were calibrated using the Bayesian Markov Chain Monte Carlo method, considering the measurement uncertainties. Based on the results of the tests and implementation, some detailed conclusions can be drawn:

- The proposed strategy can dramatically decrease unnecessary chiller switching, which commonly occurs in conventional chiller sequencing control due to measurement uncertainties and changes in operating conditions. Compared with the conventional strategy, the switching frequency was decreased by more than 54%. The life span of chillers can therefore be prolonged with reduced maintenance costs.

- The probabilistic simplified physical models calibrated using the Bayesian Markov Chain Monte Carlo method can aggregate measurement uncertainties and determine the profiles/distributions of cooling load and cooling capacity, which can be used for online risk quantification reliably.

- The proposed online stochastic decision-making scheme can effectively optimize chiller staging, to achieve energy-efficient operation of chillers and reliable thermal comfort control by providing sufficient cooling. Results showed that the total energy use of the central cooling system could be reduced by 2.8% without sacrificing thermal comfort.

It is worth noticing that, in this study, the performance of the proposed strategy was evaluated under predefined risk thresholds. The performance of the strategy under different risk thresholds should be further tested to assess their impacts on the energy efficiency and thermal comfort.

Acknowledgement

The research presented in this paper is financially supported by a general research grant (152075/19E) from the Hong Kong Research Grant Council (RGC).

Reference

[1] Yu FW, Chan KT. Improved energy management of chiller systems by multivariate and data envelopment analyses. Appl Energy 2012;92:168–74.

[2] Thangavelu SR, Myat A, Khambadkone A. Energy optimization methodology of multi-chiller plant in commercial buildings. Energy 2017;123:64–76.

[3] Liao YD. Uncertainty analysis for chiller sequencing control. Energy Build 2014;85:187–98.

[4] Huang S, Zuo WD, Sohn MD. Amelioration of the cooling load based chiller sequencing control. Appl Energy 2016;168:204–15.

[5] Sun YJ, Wang SW, Xiao F. In situ performance comparison and evaluation of three chiller sequencing control strategies in a super high-rise building. Energy Build 2013;61:333–43.

[6] Wang SW, Cui JT. Sensor-fault detection, diagnosis and estimation for centrifugal chiller systems using principal-component analysis method. Appl Energy 2005;82:197–213.

[7] Yik FWH, Chiu TW. Measuring instruments in chiller plants and uncertainties in performance evaluation. HKIE Trans 1998;5:95–9.

[8] Sun YJ, Wang SW, Huang GS. Chiller sequencing control with enhanced robustness for energy efficient operation. Energy Build 2009;41:1246–55.

[9] Huang GS, Sun YJ, Li P. Fusion of redundant measurements for enhancing the reliability of total cooling load based chiller sequencing control. Autom Constr 2011;20:789–98.

[10] Liao YD, Huang GS, Ding YF, Wu HJ, Feng ZB. Robustness enhancement for chiller sequencing control under uncertainty. Appl Therm Eng 2018;141:811–8.

[11] Yu FW, Chan KT. Experimental determination of the energy efficiency of an air-cooled chiller under part load conditions. Energy 2005;30:1747–58.

[12] Liu Z, Tan H, Luo D, Yu G, Li J, Li Z. Optimal chiller sequencing control in an office building considering the variation of chiller maximum cooling capacity. Energy Build 2017;140:430–42.

[13] Shan K, Wang SW, Gao DC, Xiao F. Development and validation of an effective and robust chiller sequence control strategy using data-driven models. Autom Constr 2016;65:78–85.

[14] Zhuang CQ, Wang SW, Shan K. Probabilistic optimal design of cleanroom air-conditioning systems facilitating optimal ventilation control under uncertainties. Appl Energy 2019;253:113576.

[15] Goel V, Grossmann IE. A stochastic programming approach to planning of offshore gas field developments under uncertainty in reserves. Comput Chem Eng 2004;28:1409–29.

[16] Hemmati R, Saboori H, Saboori S. Stochastic risk-averse coordinated scheduling of grid integrated energy storage units in transmission constrained wind-thermal systems within a conditional value-at-risk framework. Energy 2016;113:762–75.

[17] Mehdizadeh A, Taghizadegan N, Salehi J. Risk-based energy management of renewable-based microgrid using information gap decision theory in the presence of peak load management. Appl Energy 2018;211:617–30.

[18] Westermann P, Evins R. Surrogate modelling for sustainable building design–A review. Energy Build 2019;198:170–86.

[19] Zhuang CQ, Wang SW. Risk-based online robust optimal control of air-conditioning systems for buildings requiring strict humidity control considering measurement uncertainties. Appl Energy 2020.

[20] Cano EL, Moguerza JM, Alonso-Ayuso A. A multi-stage stochastic optimization model for energy systems planning and risk management. Energy Build 2016;110:49–56.

[21] Chou J-S, Ongkowijoyo CS. Risk-based group decision making regarding renewable energy

schemes using a stochastic graphical matrix model. Autom Constr 2014;37:98–109.

[22] Mavromatidis G, Orehounig K, Carmeliet J. Comparison of alternative decision-making criteria in a two-stage stochastic program for the design of distributed energy systems under uncertainty. Energy 2018;156:709–24.

[23] Li ZW, Huang GS, Sun YJ. Stochastic chiller sequencing control. Energy Build 2014;84:203–13.

[24] Gamerman D, Lopes HF. Markov chain Monte Carlo: stochastic simulation for Bayesian inference. Chapman & Hall/CRC, London; 2006.

[25] Billera LJ, Diaconis P. A geometric interpretation of the Metropolis-Hastings algorithm. Stat Sci 2001:335–9.

[26] Huang P, Augenbroe G, Huang G, Sun Y. Investigation of maximum cooling loss in a piping network using Bayesian Markov Chain Monte Carlo method. J Build Perform Simul 2019;12:117–32.

[27] Min YR, Chen Y, Yang HX. A statistical modeling approach on the performance prediction of indirect evaporative cooling energy recovery systems. Appl Energy 2019;255:113832.

[28] S.A. Klein, W.A. Beckman, J.W. Mitchell, J.A. Duffie, N.A. Duffie TLF, J.C. Mitchell et al. TRNSYS 18, a transient simulation program. University of Wisconsin-Madison, USA: Solar Energy Laboratory, 2017.

[29] Wang SW. Dynamic simulation of a building central chilling system and evaluation of EMCS on-line control strategies. Build Environ 1998;33:1–20.

[30] Ma ZJ, Wang SW. Supervisory and optimal control of central chiller plants using simplified adaptive models and genetic algorithm. Appl Energy 2011;88:198–211.

[31] HK-BEAM Society. Hong Kong Building Environmental Assessment Method: HK-BEAM Version 5/04 Existing Buildings. HK-BEAM Society; 2004. https://www.beamsociety.org.hk/files/5-04%20(full)%2021feb05.pdf (last viewed date: Sept 15, 2020).

[32] Marquardt DW. An algorithm for least-squares estimation of nonlinear parameters. J Soc Ind Appl Math 1963;11:431–41.

[33] Li Q, Augenbroe G, Brown J. Assessment of linear emulators in lightweight Bayesian calibration of dynamic building energy models for parameter estimation and performance prediction. Energy Build 2016;124:194–202.

[34] Heo Y, Choudhary R, Augenbroe GA. Calibration of building energy models for retrofit analysis under uncertainty. Energy Build 2012;47:550–60.